

Short communication

Micro Raman, FT-IR/PAS, XRD and SEM studies on glassy and partly crystalline silver phosphate ionic conductors

M. Mroczkowska^{a,*}, J.L. Nowinski^a, G.Z. Zukowska^b, A. Mroczkowska^c,
J.E. Garbarczyk^a, M. Wasiucione^a, St. Gierlotka^d^a Faculty of Physics, Warsaw University of Technology, Koszykowa 75, 00-662 Warsaw, Poland^b Faculty of Chemistry, Warsaw University of Technology, Noakowskiego 3, 00-664 Warsaw, Poland^c Department of Inorganic and Analytical Chemistry, Faculty of Pharmacy,

Medical University of Warsaw, Banacha 1, 02-097 Warsaw, Poland

^d Institute of High Pressure Physics, Polish Academy of Sciences, Sokolowska 29/37, 01-142 Warsaw, Poland

Available online 21 May 2007

Abstract

Glassy and glassy-crystalline silver ion conductors of the AgI–Ag₂O–P₂O₅ system have been studied by FTIR-PAS and Micro Raman spectroscopies in conjunction with X-ray diffractometry, scanning electron microscopy and differential scanning calorimetry. It was found out that materials with lower (≤ 60 mol%) AgI contents are fully amorphous, while those with higher contents of AgI (> 70 mol%) contain crystalline grains of β/γ -AgI embedded in the glassy matrix. Annealing of the glasses at 105 °C and/or 145 °C resulted in an increase in the formation of a yet unidentified crystalline phase dispersed in the glass. From the spectroscopic studies it was found that PO₄^{3–} units existed as separated species in the glass network or precipitated crystalline phases regardless the thermal treatment of the material. Vibrations of PO₄^{3–} units appeared to be affected by the total concentration of AgI and microstructure. The spectroscopic methods were also used to study crystallization process in the glassy samples.

© 2007 Elsevier B.V. All rights reserved.

Keywords: Micro Raman spectroscopy; Silver phosphate glasses; Ionic conductors; FTIR-PAS; Local structure

1. Introduction

In recent years most research efforts in the area of rechargeable batteries have been focused on lithium batteries, which exhibit high energy density and good cycling performance. Nevertheless there is still plenty of room for other battery systems, especially all-solid-state ones. The absence of liquid phases seems to be a precondition of any mass-scale miniaturization of on-chip power sources for modern electronics and/or MEMS devices. Silver all-solid state batteries have one important advantage over their all-solid lithium counterparts operating at room temperature – the existence of Ag⁺ – ion conducting solids with the electrical conductivity of up to 10^{–2} S cm^{–1} at ambient temperature. In the case of known lithium-based solid electrolytes the conductivity is poorer (typically 10^{–5} to 10^{–4} S cm^{–1}). Silver electrolytes exhibit also high exchange rates of electrode

reactions, which is very important for battery operation. Additionally Ag⁺ ions are the only mobile species, while in lithium polymer electrolytes most of ionic current is carried by anions. Successful and promising tests use of novel all-solid-state silver batteries with prospects of miniaturization have been reported recently by Guo et al. [1].

Silver ion conducting glasses of the AgI–Ag₂O–M_xO_y systems (M_xO_y = B₂O₃, P₂O₅, V₂O₅, etc.) exhibit high electrical conductivity (up to 10^{–2} S cm^{–1} at 25 °C) and therefore they are attractive as electrolytes for all-solid batteries or micro-batteries operating near ambient temperature [2–4]. From the viewpoint of fundamental knowledge they belong to model systems in which one can determine and explain how the high ionic conductivity of amorphous solids is related to the local structure. Despite many studies (e.g. Refs. [5–8]) the understanding of structure-ionic transport relations in these glasses is far from complete. This is partly due to a complexity of the disordered structure of the glasses [5–7] and to limited possibilities of X-ray diffractometry, the principal method of structure determination, in studies on amorphous systems.

* Corresponding author. Tel.: +48 22 234 5026; fax: +48 22 628 2171.
E-mail address: maja@if.pw.edu.pl (M. Mroczkowska).

About the local structure (basic structural units, characteristic polyhedra, symmetries, connections, etc.) one can learn using a range of spectroscopic methods such as: Raman scattering, Fourier transform-infrared absorption (FT-IR), electron paramagnetic resonance (EPR), X-ray absorption using synchrotron radiation (EXAFS and/or XANES) and others. Some of these methods, when used in their standard versions, have well-known limitations, which can be circumvented by using their specialized variants.

This work reports recent results of our investigations of the local structure of glasses and partly crystalline ionic conductors of $\text{AgI-Ag}_2\text{O-P}_2\text{O}_5$ system prepared by a standard melt-quenching. In addition some studies on the crystallization occurring in these glasses were carried out. In these studies we have used specialized spectroscopic methods: FT-IR with photoacoustic signal detection (FTIR-PAS) and Micro Raman spectroscopy. The former technique is suitable for IR studies on highly absorbing media like AgI-rich silver phosphate glasses. The advantage of this technique is also that no special sample preparation is needed [9,10]. These spectroscopic studies were carried out in conjunction with X-ray diffractometry (XRD), scanning electron microscopy (SEM) and differential scanning calorimetry (DSC). The nominal compositions of the whole series of silver phosphate materials under study were given by a cumulative formula $x\text{AgI} \cdot (100-x) (0.75\text{Ag}_2\text{O} \cdot 0.25\text{P}_2\text{O}_5)$ for $50 \leq x \leq 85$. The ratio $r = [\text{Ag}_2\text{O}]/[\text{P}_2\text{O}_5]$ between contents of a modifier (Ag_2O) and a network former (P_2O_5) was fixed to 3. Such a high r -value means that the phosphate glass network is considerably disrupted by the modifier. In consequence $r=3$ determines what structural units are likely to be present in the material and in what proportions.

2. Experimental

Glasses of nominal compositions given by a formula $x\text{AgI} (100-x) (0.75\text{Ag}_2\text{O} \cdot 0.25\text{P}_2\text{O}_5)$ for $50 \leq x \leq 85$ were prepared by a standard melt quenching technique [11]. Selected samples were annealed at temperatures 105 or 145 °C, in order to promote and/or accelerate their crystallization. The as-prepared and thermally treated samples were examined by X-ray diffractometry on a Philips X'Pert Pro diffractometer ($\text{Cu K}\alpha$ radiation, $\lambda = 1.54 \text{ \AA}$). Micro Raman investigations were carried out at room temperature using a Nicolet Almega XR spectrometer. A low energy 785 nm line was used for excitation. The spectral resolution was better than 2 cm^{-1} . A part of spectra were acquired in the polarization mode to enable identification of the Raman bands. Infrared spectra (FTIR-PAS) were collected in mid-IR region $400\text{--}4000 \text{ cm}^{-1}$ on a Perkin-Elmer Spectrum 1000 spectrometer with a MCT 300 detector. Presence (or absence) of thermal events, corresponding to glass transition, crystallization and/or melting of the studied samples was investigated by differential scanning calorimetry (DSC) using a Perkin-Elmer Pyris 1 calorimeter. The scans were acquired in the $20\text{--}540 \text{ }^\circ\text{C}$ temperature range at 20 K min^{-1} heating rate. Microstructure was observed by field-emission scanning electron microscopy (FE-SEM) using a LEO 1530 setup.

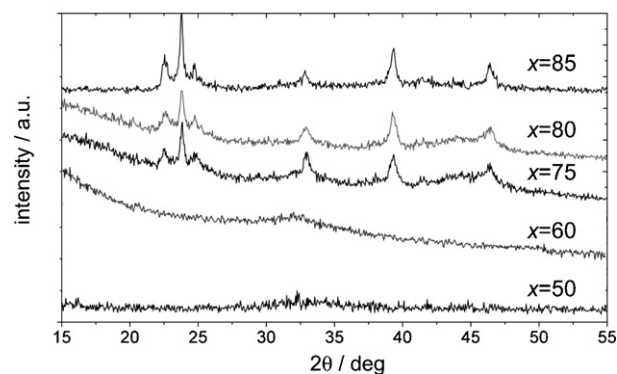


Fig. 1. X-ray diffraction patterns for as-received samples of compositions given by $x = 50, 60, 75, 80$ and 85 . Peaks visible in the patterns for $x = 75, 80$ and 85 correspond to $\beta/\gamma\text{-AgI}$.

3. Results and discussion

3.1. Studies on as-prepared materials

The XRD patterns of the as-received samples are shown in Fig. 1. For samples with $x \leq 60$ one sees only a wide ‘halo’ typical for amorphous materials. For materials with $x > 70$ one observes distinct diffraction lines corresponding to $\beta/\gamma\text{-AgI}$ crystalline phases. The corresponding SEM micrographs of freshly cleaved surfaces show that the glasses with $x \leq 60$ are characterized by a continuous uniform microstructure with no foreign phases (Fig. 2a). On the contrary, the microstructure of the samples corresponding to $x > 70$ is inhomogeneous and contains numerous inclusions of about $1 \text{ }\mu\text{m}$ in size (Fig. 2b).

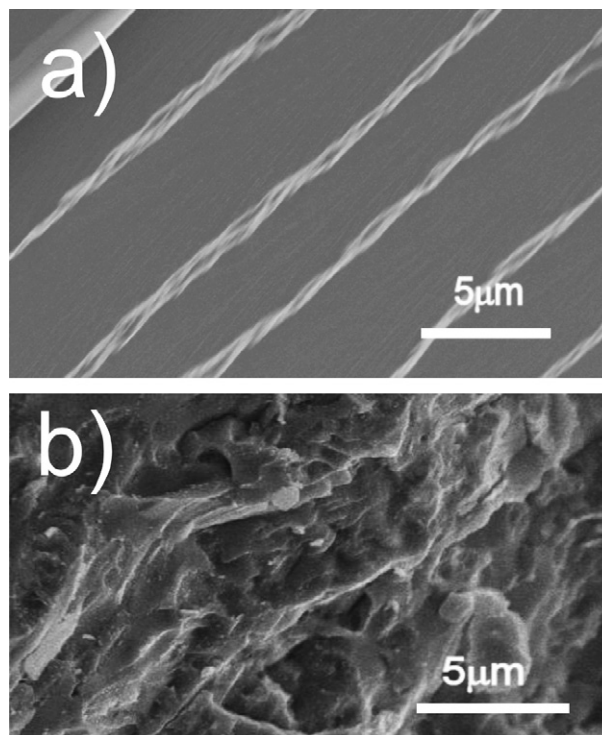


Fig. 2. SEM images of cleaved surfaces of as-received materials of compositions corresponding to $x = 60$ (a) and $x = 80$ (b).

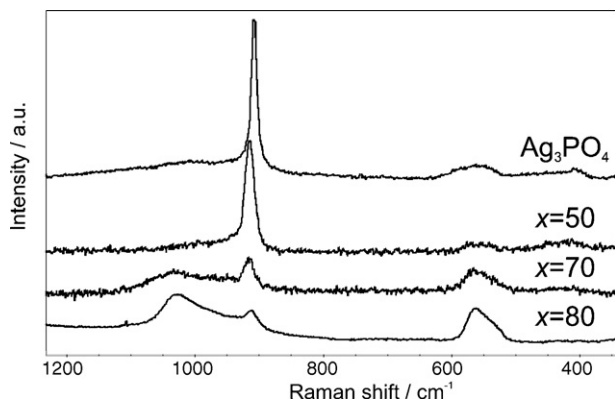


Fig. 3. Raman spectra of as-received materials of compositions corresponding to $x = 50, 70$ and 80 . A spectrum of silver phosphate is given for comparison.

The results of both XRD and SEM characterization of the as-received materials show that for lower AgI contents ($x \leq 60$) they are fully amorphous and for $x > 70$ they contain crystalline grains (mainly of β/γ AgI) embedded in amorphous matrix.

The Raman spectra for the selected materials with $x = 50, 70$ and 80 are presented in Fig. 3. For the composition $x = 50$ one can see weak bands centered at: $422, 557$ and 979 cm^{-1} and a very strong one at 914 cm^{-1} . All these bands are characteristic for the oscillations of PO_4^{3-} groups possessing a T_d symmetry [12,13]. A similar spectrum was observed for Ag_3PO_4 (upper curve in Fig. 3). The most intense band at 914 cm^{-1} corresponds to the ν_1 symmetric stretching vibration of the P–O bonds [14,15]. This assignment is strongly supported by the fact that this band is substantially suppressed, when measured in the polarization mode [15]. Two bands – at 422 and 557 cm^{-1} – are both assigned to bending vibrations of PO_4^{3-} , whereas that at 979 cm^{-1} to an asymmetrical stretching vibration [12,13,15,16]. Fig. 4 shows a deconvoluted Raman spectrum of the as-received glass corresponding to $x = 50$. The assignments of the particular vibration modes are given in Fig. 4. From Figs. 3 and 4 it is clear that the positions of the bands of as-prepared samples of different compositions remain basically the same, but their intensities vary from composition to composition. This indicates that the frequencies of the vibration modes are insensitive to the changes in the AgI content. On the other hand quite strong intensity variations among samples with different x can be attributed

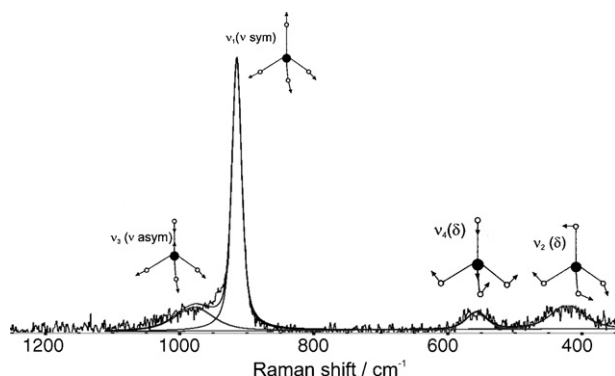


Fig. 4. The deconvoluted Raman spectrum for the glass with $x = 50$. Raman intensity is given in arbitrary units.

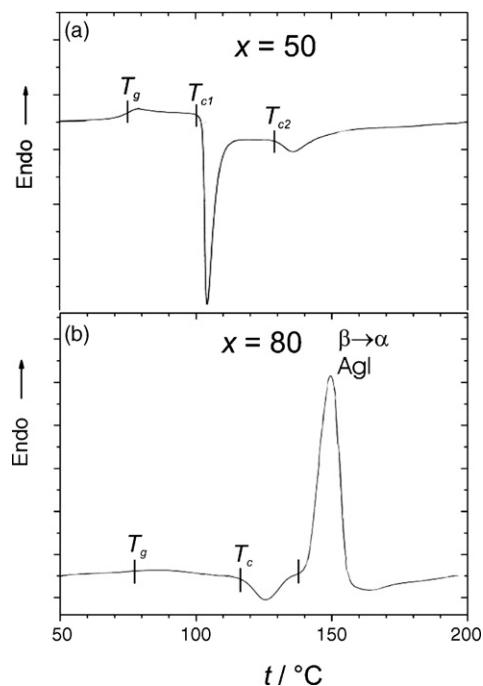


Fig. 5. DSC traces for samples with $x = 50$ (a) and $x = 80$ (b). The scans were taken at 20 K min^{-1} heating rate.

to the effects of departure from the original high symmetry. In the case of PO_4^{3-} tetrahedra a departure from their original T_d symmetry leads to an increase in the intensity of certain vibration modes, especially the asymmetric ones. The observed changes in relative intensities of the Raman bands clearly indicate that AgI dopant has an effect on the symmetry of the PO_4^{3-} tetrahedra.

The DSC traces of all as-prepared materials exhibited an endothermic feature near and below 80°C , assigned to a glass transition. Two examples of DSC curves, for samples with $x = 50$ and 80 , are shown in Fig. 5. For compositions with lower AgI contents ($x = 50$) one can see a baseline shift at ca $T_g = 80^\circ\text{C}$ followed by a strong exothermic peak starting at $T_{c1} \approx 100^\circ\text{C}$ (Fig. 5a). The peak is due to the irreversible crystallization process. Another weaker exothermic peak is visible at ca 130°C . The temperature T_{c1} of the first crystallization peak decreased with x for compositions until $x = 75$. Above $x = 80$ it increased anew. For the materials characterized by $x \geq 80$ (Fig. 5b), a feature related to the glass transition is hardly visible suggesting low glass contents in the material. At higher temperatures there is a weak exothermic peak at ca. 120°C , indicating crystallization phenomena. A strong endothermic peak was observed at around 150°C . In a natural way it was assigned to the reversible $\beta \rightarrow \alpha$ phase transition of the silver iodide, since it is known that for bulk AgI this transition takes place at 147°C [17].

3.2. Studies on thermally treated materials

The materials of compositions corresponding to $x = 50$ and 80 were selected for the studies on the crystallization induced by thermal processing. The former material (i.e. $x = 50$) was annealed first at 105°C for 20 min to investigate the initial stages

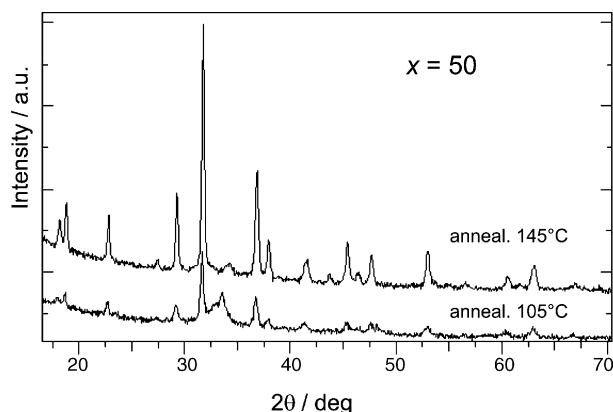


Fig. 6. Room temperature X-ray diffraction patterns for a sample with $x = 50$ after annealing: at 105 °C (lower pattern) and at 145 °C (upper curve).

of crystallization and then additionally at 145 °C, also for 20 min. In the case of the samples with $x = 80$, the annealing at only one temperature 145 °C for 20 min was carried out.

XRD patterns of the material corresponding to $x = 50$ after annealing at 105 °C (lower curve) and 145 °C (upper curve), are shown in Fig. 6. The as-received material of that composition was amorphous (see Fig. 1). The observed changes indicate that the 1st annealing at 105 °C (which is higher than T_g for that glass) leads to the appearance of crystalline grains of phase yet unidentified by us. The second annealing, this time at 145 °C, causes an increase in the intensity of these peaks but also leads to the appearance of some other lines.

Fig. 7 shows IR spectra of the materials of compositions corresponding to $x = 50$, 70 and 75. For each material there are two spectra: one for the as-received sample and one for the same sample annealed at 105 °C for 20 min. One can see broad bands at 800–1150 and the 460–640 cm^{-1} . They have been assigned to the asymmetric stretching modes and bending ones, respectively. Interesting fact is a presence of the absorbance band near 911 cm^{-1} which is visible in as-received sample spectra. The band is due to ν_1 —symmetric stretching vibration of PO_4^{3-} and for T_d symmetry molecules it should be IR inactive. It may be IR activated only under special conditions, e.g. in presence of

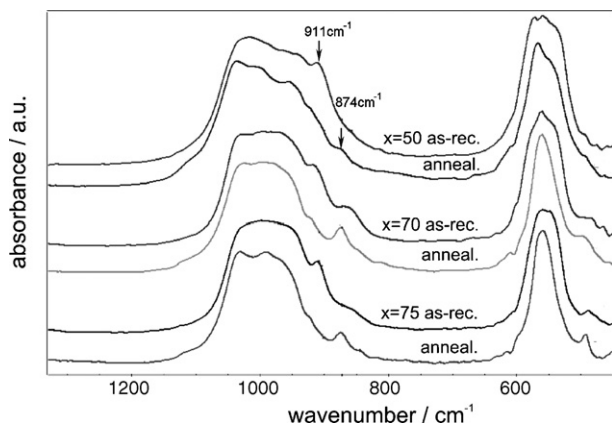


Fig. 7. FTIR-PAS spectra for as-received and annealed samples of compositions corresponding to $x = 50$ (top curves), $x = 70$ (middle curves) and $x = 75$ (bottom curves).

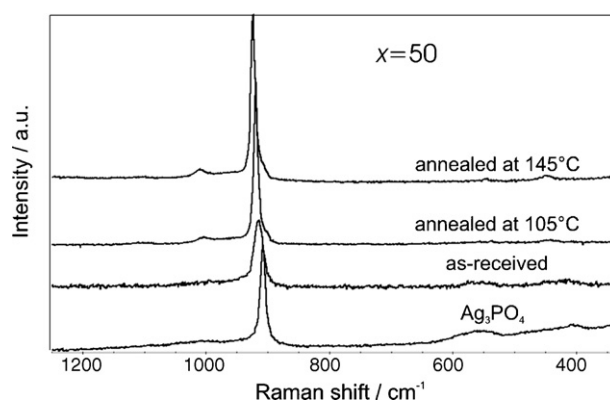


Fig. 8. Room temperature Raman spectra of samples of composition corresponding to $x = 50$: as-received, annealed at 105 °C for 20 min and annealed at 145 °C for 20 min. As a reference the spectrum of silver phosphate is included (bottom curve).

heavy polarisable cation (like Ag^+) due to its distorting influence on tetrahedron [18].

In IR spectra of annealed samples (Fig. 7) 911 cm^{-1} band becomes less important. These results suggest weakening distortion effect of the surrounding silver ions on PO_4^{3-} tetrahedra. It seems that the change of the local distribution of these ions, like ordering, is responsible for the effect. A new band visible at 874 cm^{-1} appears. Its origin is unclear. Some authors (e.g. Ref. [19]) attribute the band to the ν_1 symmetric vibration mode of a PO_4^{3-} tetrahedron in a crystal field.

Interesting changes were observed in Raman spectra of the thermally treated samples. In the case of the glass corresponding to $x = 50$ one can see an increase in the intensity of the band near 914 cm^{-1} as a result of annealing (Fig. 8). Moreover the position of this band (and of other bands) slightly shifts towards higher energies and its width decreases. Such a tendency indicates some ordering of structural units. An additional effect of the annealing on the spectra is the appearance of a weak band at ca. 1010 cm^{-1} .

More striking is the difference between spectra of as-received and annealed sample of composition corresponding to $x = 80$ (Fig. 9). For the as-received sample one can see broad bands of

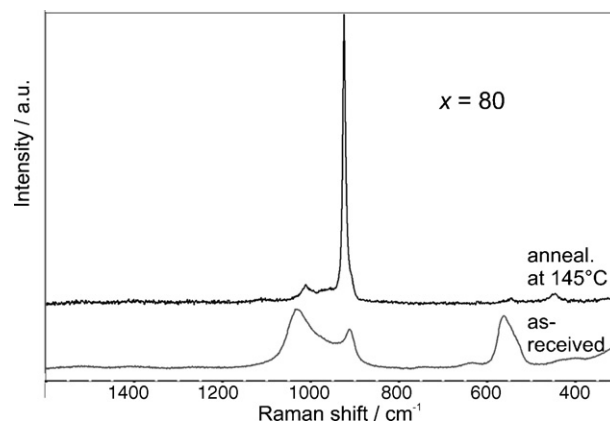


Fig. 9. Room temperature Raman spectra of samples of composition corresponding to $x = 80$: as-received (lower curve) and annealed at 145 °C for 20 min (upper curve).

comparable intensity, centered at 570, 914 and 1040 cm^{-1} and some additional much weaker features. After heat treatment at 145 °C the intensity of the 914 cm^{-1} band becomes much higher and dominates all other features. The spectrum reminds that of an annealed sample with $x=50$ (cf. Fig. 8). Such a similarity suggests that the additional crystallization of the material with very high AgI content also resulted in some ordering of the PO_4^{3-} units.

4. Conclusions

Our FTIR-PAS and Micro Raman spectroscopic studies have shown the changes in the local structure of the materials under study, caused by various AgI contents. It was pointed out that there is an abundance of free PO_4^{3-} units in a glassy matrix. These tetrahedral PO_4^{3-} units could be distorted due to presence of large, polarisable cations (Ag^+) in their vicinity. It was found out that materials with very high AgI contents ($x > 70$) consist of two components: glass and crystalline β/γ -AgI grains. The DSC investigation showed that for $x \leq 60$ initially amorphous materials underwent crystallization when thermally treated at temperatures higher than T_g . This phenomenon was confirmed by scanning electron microscopy and XRD experiments. The annealing leads to changes in Raman spectra: a slight shift of the strongest narrow band at ca 914 cm^{-1} and its narrowing. These changes have been ascribed to the effect of newly formed crystalline phases on basic constituting units of the phosphate network. The Raman investigations of the studied materials also suggested, that rearrangement of structure units of the glass during crystallization did not involve linking of PO_4^{3-} tetrahedra.

References

- [1] Y.-G. Guo, Y.-S. Hu, J.-S. Lee, J. Maier, *Electrochem. Commun.* 8 (2006) 1179–1184.
- [2] C.A. Angell, *Annu. Rev. Phys. Chem.* 43 (1992) 693–717.
- [3] T. Minami, B.V.R. in: S. Chowdari, Radhakrishna (Eds.), *Materials for Solid State Batteries*, World Scientific, Singapore, 1986.
- [4] J.E. Garbarczyk, P. Jozwiak, M. Wasiucionek, J.L. Nowinski, *Solid State Ionics* 175 (2004) 691–694.
- [5] T. Minami, T. Katsuda, M. Tanaka, *J. Phys. Chem.* 83 (1979) 1306–1309.
- [6] R. Bacewicz, P. Woroniecki, J. Garbarczyk, *Phys. Chem. Glasses* 40 (1999) 175–176.
- [7] T. Minami, Y. Takuma, M. Tanaka, *J. Electrochem. Soc.* 124 (1977) 1659–1662.
- [8] J.W. Zwanziger, K.K. Olsen, S.L. Tagg, *Phys. Rev. B* 47 (1993) 14618–14621.
- [9] S.E. Bialkowski, *Photothermal Spectroscopy Methods for Chemical Analysis*, vol. 134 in *Chemical Analysis: A Series of Monographs on Analytical Chemistry and its Applications*, J.D. Winefordner, Series Editor, J. Wiley, New York, 1996.
- [10] D.P. Almond, P.M. Patel, *Photothermal Science and Techniques*, Chapman & Hall, London, 1996.
- [11] J.L. Nowinski, M. Mroczkowska, J. Dygas, J.E. Garbarczyk, M. Wasiucionek, *Solid State Ionics* 176 (2005) 1775–1779.
- [12] K. Nakamoto, *Infrared and Raman Spectra of Inorganic and Coordination Compounds*, John Wiley & Sons Inc., New York, 1997.
- [13] R.A. Nyquist, C.L. Putzig, M.A. Leugers, *Infrared and Raman Spectral Atlas of Inorganic Compounds and Organic Salts: Raman Spectra*, Academic Press, San Diego, 1997.
- [14] W.L. Marshall, G.M. Begun, *J. Chem. Soc.* 85 (1989) 1963–1978.
- [15] C.M. Preston, W.A. Adams, *J. Phys. Chem.* 83 (1979) 814–821.
- [16] A. Ait Salah, P. Jozwiak, J. Garbarczyk, K. Benkhoulja, K. Zaghib, F. Gendron, C.M. Julien, *J. Power Sources* 140 (2005) 370–375.
- [17] L.W. Strock, *Z. Phys. Chem. B* 25 (1934) 441–459.
- [18] D.E.C. Corbridge, E.J. Lowe, *J. Chem. Soc.* (1954) 493–502.
- [19] A. Ghule, R. Murugan, H. Chang, *Inorg. Chem.* 40 (2001) 5917–5923.